PHYSICAL REVIEW D **84,** 036011 (2011)

Thermodynamics of quark quasiparticle ensemble

S. V. Molodtsov*
Joint Institute for Nuclear Research, Dubna, Moscow Region, Russia

G. M. Zinovjev
Bogolyubov Institute for Theoretical Physics, National Academy of Sciences of Ukraine, Kiev, Ukraine
(Received 30 March 2011; published 22 August 2011)

The features of the hot and dense gas of quarks, which are considered as the quasiparticles of the model Hamiltonian with a four-fermion interaction, are studied. Being adapted to the Nambu–Jona-Lasinio model, this approach allows us to accommodate a phase transition similar to the nuclear liquid-gas one at the proper scale and to argue the existence of the mixed (inhomogeneous) phase of vacuum and normal baryonic matter as a plausible scenario of chiral symmetry (partial) restoration. Analyzing the transition layer between two phases, we estimate the surface tension coefficient and speculate on the possible existence of a quark droplet.

DOI: 10.1103/PhysRevD.84.036011 PACS numbers: 11.10.−z, 11.15.Tk

I. INTRODUCTION

Notwithstanding the well-known incompletion of quantum chromodynamics and its strongly limited capacity to perform the nonperturbative calculations both in the vacuum and at finite temperature and baryonic density, one of the major predictions of this theory, the possible existence of quark-gluon plasma, was so exciting and convincing that it pushed forward a very active research programme in experiments with relativistic heavy ions. In such a situation when the applications which should usually be based on the standard interrelations between the hadronic properties and the QCD Lagrangian parameters are merely impossible, but the practical need in the quantitative estimates is dictated by the running experiments, we are forced to be very peristent and pragmatic in searching the effective Lagrangians.

The Nambu–Jona-Lasinio (NJL) model and its numerous extensions are the most popular in this context because they share some global symmetries of QCD and allow us to make some serious difficulties and uncertainties faced in the QCD calculations surmountable. It appears especially appreciable and effective in studying the nature of nuclear matter with its (super)dense state being treated as a model of QCD at large quark chemical potential. Nowadays, experiments in heavy-ion collisions, to a considerable extent, are driven by the results of phenomenological investigations of the properties of nucleon-nucleon force and the phase diagram of strongly interacting matter which relies on the corresponding estimates of experimentally measurable quantities.

Thus, exploring the QCD phase diagram with the effective models is targeted from the theoretical view point by the necessity to find out some kind of interpolation between the physics as conceived by the lattice QCD simulations (still unrealistic for several reasons) and the physics outputs of phenomenological studies. The vast activity (and progress) along this line [1], together with the recent experimental results from the LHC and the Relativistic Heavy Ion Collider [2], leads to the unexpected vision of still pending questions and, perhaps, their new interpretation.

These and some related topics are discussed in this paper, inspired by the well-known and fruitful idea about the specific role of surface degrees of freedom in the finite Fermi-liquid systems [3] and, to a considerable extent, by our previous works [4,5] in which the quarks were treated as the quasiparticles of the model Hamiltonian, and the problem of filling up the Fermi sphere was studied in detail. In particular, within the NJL model [6] new solution branches of the equation for dynamical quark mass as a function of chemical potential (the details are shown below in Fig. 1) have been found. Besides, the existence and origin of the state filled up with quarks, which is almost degenerate with the vacuum state both in the quasiparticle chemical potential and in the ensemble pressure, has been demonstrated. In general, the approach developed may be considered as another microscopical substantiation of the bag model in which the states filled up with quarks might be instrumental as a ''construction material'' for baryons.

Our analysis here is performed within two approaches which are complementary, in a sense, but, fortunately, lead to identical results. One of these approaches, based on the Bogolyubov transformation, is especially informative for studying the process of filling up the Fermi sphere because the density of the quark ensemble develops a continuous dependence on the Fermi momentum in this case. It allows us to reveal an additional structure in the solution of the gap equation for dynamical quark mass just in the proper interval of parameters characteristic for the phase transition, and to trace its evolution. It results in the possibility for the quark (fermionic) ensemble to be found in two aggregate states, a gas and a liquid, and in the partial

*Also at Institute of Theoretical and Experimental Physics, Moscow, Russia.

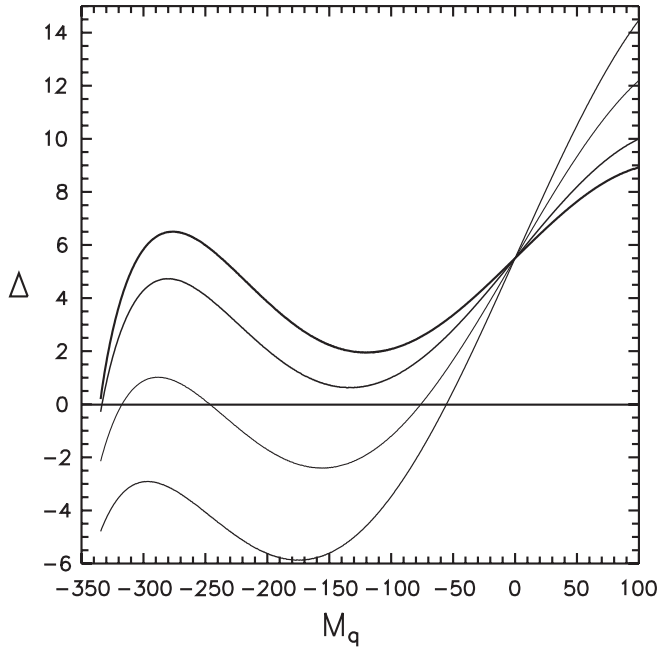

FIG. 1. The residual Δ for Eq. (15) is presented as a function of dynamical quark mass M_q (MeV) at zero temperature and the following values of chemical potential μ (MeV)—335 (the lowest curve), 340, 350, 360 (the top curve).

restoration of chiral the condensate in a liquid phase (Sec. II). In order to make these conclusions easily perceptible, we deal with the simplest version of the NJL model (with one flavor and one of the standard parameter sets). We also try to construct a description of the transition layer between the two phases and, in particular, to estimate the surface tension coefficient (Sec. III) that is of obvious importance in the context of discussing the possible quark droplet formation (Sec. IV). Some technical moments of calculating the mean energy functional are given in the Appendix.

II. EXPLORING THE QUARK ENSEMBLE

Now, as an input for starting, we note the key elements of the approach which has been developed in [4,5]. The corresponding model Hamiltonian includes the interaction term taken in the form of a product of two color currents located in the spatial points $\mathbf{x}$ and $\mathbf{y}$ which are connected by a form factor, and its density reads

$$\mathcal{H} = -\bar{q}(i\boldsymbol{\gamma}\boldsymbol{\nabla} + im)q - \bar{q}t^a\gamma_\mu q \int d\mathbf{y}\bar{q}'t^b\gamma_\nu q'\langle A^a_\mu A'^b_\nu\rangle, \tag{1}$$

where $q = q(\mathbf{x})$, $\bar{q} = \bar{q}(\mathbf{x})$, $q' = q(\mathbf{y})$, $\bar{q}' = \bar{q}(\mathbf{y})$ are the quark and antiquark operators,

$$q_{\alpha i}(\mathbf{x}) = \int \frac{d\mathbf{p}}{(2\pi)^3}\frac{1}{(2|p_4|)^{1/2}}[a(\mathbf{p}, s, c)u_{\alpha i}(\mathbf{p}, s, c)e^{i\mathbf{px}} + b^+(\mathbf{p}, s, c)v_{\alpha i}(\mathbf{p}, s, c)e^{-i\mathbf{px}}], \tag{2}$$

where $p_4^2 = -\mathbf{p}^2 - m^2$; i is the color index; α is the spinor index in the coordinate space; a^+, a and b^+, b are the creation and annihilation operators of quarks and antiquarks; $a|0\rangle = 0$; $b|0\rangle = 0$; $|0\rangle$ is the vacuum state of the free Hamiltonian; and m is the current quark mass. The summation over indices s and c is meant everywhere, the index s describes two spin polarizations of the quark, and the index c plays a similar role for the color. As usual, $t^a = \lambda^a/2$ are the generators of the $SU(N_c)$ color gauge group. The Hamiltonian density is considered in Euclidean space, and γ_μ denote the Hermitian Dirac matrices, μ, $\nu = 1, 2, 3, 4$. $\langle A^a_\mu A'^b_\nu\rangle$ stands for the form factor of the following form:

$$\langle A^a_\mu A'^b_\nu\rangle = \delta^{ab}\frac{2\tilde{G}}{N_c^2 - 1}[I(\mathbf{x} - \mathbf{y})\delta_{\mu\nu} - J_{\mu\nu}(\mathbf{x} - \mathbf{y})], \tag{3}$$

where the second term is spanned by the relative distance vector and the gluon field primed denotes that in the spatial point $\mathbf{y}$. The effective Hamiltonian density (1) results from averaging the ensemble of quarks influenced by the intensive stochastic gluon field A^a_μ; see Ref. [4]. For the sake of simplicity, we neglect the contribution of the second term in (3) in what follows. The ground state of the system is searched as the Bogolyubov trial function composed of the quark-antiquark pairs with opposite momenta and with vacuum quantum numbers, i.e.

$$|\sigma\rangle = \mathcal{T}|0\rangle,$$
$$\mathcal{T} = \Pi_{p,s}\exp\{\varphi[a^+(\mathbf{p}, s)b^+(-\mathbf{p}, s) + a(\mathbf{p}, s)b(-\mathbf{p}, s)]\}. \tag{4}$$

In this formula and below, in order to simplify the notations, we refer to one compound index only, which means both the spin and color polarizations. The parameter $\varphi(\mathbf{p})$ which describes the pairing strength is determined by the minimum of mean energy,

$$E = \langle\sigma|H|\sigma\rangle. \tag{5}$$

By introducing the "dressing transformation" we define the creation and annihilation operators of quasiparticles as $A = \mathcal{T}a\mathcal{T}^{-1}$, $B^+ = \mathcal{T}b^+\mathcal{T}^{-1}$ and for fermions $\mathcal{T}^{-1} = \mathcal{T}^\dagger$. Then the quark field operators are presented as

$$q(\mathbf{x}) = \int \frac{d\mathbf{p}}{(2\pi)^3}\frac{1}{(2|p_4|)^{1/2}}[A(\mathbf{p}, s)U(\mathbf{p}, s)e^{i\mathbf{px}} + B^+(\mathbf{p}, s)V(\mathbf{p}, s)e^{-i\mathbf{px}}],$$
$$\bar{q}(\mathbf{x}) = \int \frac{d\mathbf{p}}{(2\pi)^3}\frac{1}{(2|p_4|)^{1/2}}[A^+(\mathbf{p}, s)\bar{U}(\mathbf{p}, s)e^{-i\mathbf{px}} + B(\mathbf{p}, s)\bar{V}(\mathbf{p}, s)e^{i\mathbf{px}}],$$

and the transformed spinors U and V are given by the following forms:

$$U(\mathbf{p}, s) = \cos(\varphi)u(\mathbf{p}, s) - \sin(\varphi)v(-\mathbf{p}, s),$$
$$V(\mathbf{p}, s) = \sin(\varphi)u(-\mathbf{p}, s) + \cos(\varphi)v(\mathbf{p}, s), \quad (6)$$

where $\bar{U}(\mathbf{p}, s) = U^+(\mathbf{p}, s)\gamma_4$, $\bar{V}(\mathbf{p}, s) = V^+(\mathbf{p}, s)\gamma_4$ are the Dirac conjugated spinors.

In Ref. [5] the process of filling in the Fermi sphere with the quasiparticles of quarks was studied by constructing the state of the Sletter determinant type

$$|N\rangle = \prod_{|\mathbf{P}|<P_F;S} A^+(\mathbf{P}; S)|\sigma\rangle, \quad (7)$$

which possesses the minimal mean energy over the state $|N\rangle$. The polarization indices run through all permissible values here, and the quark momenta are bounded by the limiting Fermi momentum P_F. The momenta and polarizations of states forming the quasiparticle gas are marked by capital letters, similar to the above formula, and the small letters are used in all other cases.

As it is known, the ensemble state at finite temperature T is described by the equilibrium statistical operator ξ. Here we use the Bogolyubov-Hartree-Fock approximation in which the corresponding statistical operator is presented by the following form:

$$\xi = \frac{e^{-\beta\hat{H}_{\text{app}}}}{Z_0}, \qquad Z_0 = \text{Tr}\{e^{-\beta\hat{H}_{\text{app}}}\}, \quad (8)$$

where an approximating effective Hamiltonian H_{app} is quadratic in the creation and annihilation operators of quark and antiquark quasiparticles A^+, A, B^+, B, and is defined in the corresponding Fock space with the vacuum state $|\sigma\rangle$ and $\beta = T^{-1}$. There is no need to know the exact form of this operator, henceforth, because all the quantities of our interest in the Bogolyubov-Hartree-Fock approximation are expressed by the corresponding averages $n(P) = \text{Tr}\{\xi A^+(\mathbf{P}; S)A(\mathbf{P}; S)\}$, $\bar{n}(Q) = \text{Tr}\{\xi B^+(\mathbf{Q}; T)B(\mathbf{Q}; T)\}$ which are obtained by solving the following variational problem. The statistical operator ξ is defined by such a form in order to have the minimal value of mean energy of the quark ensemble,

$$E = \text{Tr}\{\xi H\},$$

at the fixed mean charge

$$\bar{Q}_4 = \text{Tr}\{\xi Q_4\} = V2N_c \int \frac{d\mathbf{p}}{(2\pi)^3}[n(p) - \bar{n}(p)], \quad (9)$$

where

$$Q_4 = -\int d\mathbf{x}\bar{q}i\gamma_4 q = \int \frac{d\mathbf{p}}{(2\pi)^3}\frac{-ip_4}{|p_4|}[A^+(p)A(p) + B(p)B^+(p)],$$

for the diagonal component (which is a point of interest here) and at the fixed mean entropy ($S = -\ln\xi$),

$$\bar{S} = -\text{Tr}\{\xi\ln\xi\} = -V2N_c\int\frac{d\mathbf{p}}{(2\pi)^3}[n(p)\ln n(p) + (1-n(p))\ln(1-n(p)) + +\bar{n}(p)\ln\bar{n}(p) + (1-\bar{n}(p))\ln(1-\bar{n}(p))]. \quad (10)$$

The mean charge (9) is calculated here up to the unessential (infinite) constant coming from permuting the operators BB^+ in the charge operator Q_4. It is appropriate here to note that the mean charge should be treated in some statistical sense because it characterizes the quark ensemble density and has no color indices. The mean energy density per one quark degree of freedom $w = \mathcal{E}/(2N_c)$, $\mathcal{E} = E/V$, where E is the total energy of the ensemble calculated (the details of derivation can be found in the Appendix) to get the following form:

$$w = \int\frac{d\mathbf{p}}{(2\pi)^3}|p_4| + \int\frac{d\mathbf{p}}{(2\pi)^3}|p_4|\cos\theta[n + \bar{n} - 1] - G \times\int\frac{d\mathbf{p}}{(2\pi)^3}\sin(\theta - \theta_m)[n + \bar{n} - 1] \times\int\frac{d\mathbf{q}}{(2\pi)^3}\sin(\theta' - \theta'_m)[n' + \bar{n}' - 1]I, \quad (11)$$

where $\theta = 2\varphi$, $\theta' = \theta(q)$, $n' = n(q)$, $I = I(\mathbf{p} + \mathbf{q})$, and the angle $\theta_m(p)$ is determined by $\sin\theta_m = m/|p_4|$. We are interested in minimizing the following functional:

$$\Omega = E - \mu\bar{Q}_4 - T\bar{S}, \quad (12)$$

where μ and T are the Lagrange factors for the chemical potential and temperature, respectively. The approximating Hamiltonian $\hat{H}_{\text{app}}$ is constructed simply by using the information on $E - \mu\bar{Q}_4$ of the presented functional (see also below). For the specific contribution per one quark degree of freedom $f = F/(2N_c)$, $F = \Omega/V$, we obtain

$$f = \int\frac{d\mathbf{p}}{(2\pi)^3}[|p_4|\cos\theta(n + \bar{n} - 1) - \mu(n - \bar{n})] + \int\frac{d\mathbf{p}}{(2\pi)^3}|p_4| - G\int\frac{d\mathbf{p}}{(2\pi)^3}\sin(\theta - \theta_m)(n + \bar{n} - 1) \times\int\frac{d\mathbf{q}}{(2\pi)^3}\sin(\theta' - \theta'_m)(n' + \bar{n}' - 1)I + T \times\int\frac{d\mathbf{p}}{(2\pi)^3}[n\ln n + (1-n)\ln(1-n) + \bar{n}\ln\bar{n} + (1-\bar{n})\ln(1-\bar{n})]. \quad (13)$$

The optimal values of the parameters are determined by solving the following system of equations ($df/d\theta = 0$, $df/dn = 0$, $df/d\bar{n} = 0$):

$$|p_4|\sin\theta - M\cos(\theta - \theta_m) = 0,$$
$$|p_4|\cos\theta - \mu + M\sin(\theta - \theta_m) - T\ln(n^{-1} - 1) = 0,$$
$$|p_4|\cos\theta + \mu + M\sin(\theta - \theta_m) - T\ln(\bar{n}^{-1} - 1) = 0, \quad (14)$$

where we denoted the induced quark mass as

$$M(\mathbf{p}) = 2G \int \frac{d\mathbf{q}}{(2\pi)^3}(1 - n' - \bar{n}')\sin(\theta' - \theta'_m)I(\mathbf{p} + \mathbf{q}). \tag{15}$$

Turning to the presentation of the obtained results in the form customary for the mean field approximation, we introduce a dynamical quark mass M_q parametrized as

$$\sin(\theta - \theta_m) = \frac{M_q}{|P_4|}, \qquad |P_4| = (\mathbf{p}^2 + M_q^2(\mathbf{p}))^{1/2}, \tag{16}$$

and ascertain the interrelation between induced and dynamical quark masses. From the first equation of system (14), we fix the pairing angle

$$\sin\theta = \frac{pM}{|p_4||P_4|}$$

and, making use of the identity

$$(|p_4|^2 - Mm)^2 + M^2p^2 = [p^2 + (M - m)^2]|p_4|^2, \tag{17}$$

we find out that

$$\cos\theta = \pm\frac{|p_4|^2 - mM}{|p_4||P_4|}.$$

For the sake of clarity, we choose the upper sign to be ''plus.'' Then, as an analysis of the NJL model teaches, the branch of the equation solution for negative dynamical quark mass is the most stable one. Let us remember here that we are dealing with the Euclidean metrics (though it is not a principal point), and a quark mass appears in the corresponding expressions as an imaginary quantity. Now, substituting the calculated expressions for the pairing angle into the trigonometrical factor

$$\sin(\theta - \theta_m) = \sin\theta\frac{p}{|p_4|} - \cos\theta\frac{m}{|p_4|}$$

and performing some algebraic transformations, we get the relation

$$M_q(\mathbf{p}) = M(\mathbf{p}) - m. \tag{18}$$

In particular, the equation for dynamical quark mass (15) gets the form characteristic of the mean field approximation,

$$M = 2G \int \frac{d\mathbf{q}}{(2\pi)^3}(1 - n' - \bar{n}')\frac{M'_q}{|P'_4|}I(\mathbf{p} + \mathbf{q}). \tag{19}$$

The second and third equations of system (14) allow us to find the following expressions,

$$n = (e^{\beta(|P_4| - \mu)} + 1)^{-1}, \qquad \bar{n} = (e^{\beta(|P_4| + \mu)} + 1)^{-1}, \tag{20}$$

and, hence, the thermodynamic properties of our system, in particular, the pressure of the quark ensemble,

$$P = -\frac{dE}{dV}.$$

By definition, we should calculate this derivative at constant mean entropy, $d\bar{S}/dV = 0$. This condition makes it possible, for example, to calculate the derivative $d\mu/dV$, but the mean charge $\bar{Q}_4$ should not change. In order to maintain its validity, we introduce two independent chemical potentials—for quarks μ and for antiquarks $\bar{\mu}$ [following Eq. (20) with the opposite signs]. This also leads to the change $\mu \to \bar{\mu}$ in the definition of $\bar{n}$ in Eq. (20). This kind of description apparently allows us to treat even some nonequilibrium states of the quark ensemble (but losing a covariance similar to the situation which takes place in electrodynamics while one deals with electron-positron gas). Here we are interested in the unaffected balanced situation of $\bar{\mu} = \mu$. Then the corresponding derivative of specific energy dw/dV might be presented as

$$\frac{dw}{dV} = \int \frac{d\mathbf{p}}{(2\pi)^3}\left(\frac{dn}{d\mu}\frac{d\mu}{dV} + \frac{d\bar{n}}{d\bar{\mu}}\frac{d\bar{\mu}}{dV}\right) \times \left[|p_4|\cos\theta - 2G\sin(\theta - \theta_m) \times \int \frac{d\mathbf{q}}{(2\pi)^3}\sin(\theta' - \theta'_m)(n' + \bar{n}' - 1)I\right].$$

Now, representing the trigonometric factors via dynamical quark mass and drawing Eq. (15), we obtain, for the ensemble pressure,

$$P = -\frac{E}{V} - V2N_c \int \frac{d\mathbf{p}}{(2\pi)^3}\left(\frac{dn}{d\mu}\frac{d\mu}{dV} + \frac{d\bar{n}}{d\bar{\mu}}\frac{d\bar{\mu}}{dV}\right)|P_4|. \tag{21}$$

The requirement of mean charge conservation,

$$\frac{d\bar{Q}_4}{dV} = \frac{\bar{Q}_4}{V} + V2N_c \int \frac{d\mathbf{p}}{(2\pi)^3}\left(\frac{dn}{d\mu}\frac{d\mu}{dV} - \frac{d\bar{n}}{d\bar{\mu}}\frac{d\bar{\mu}}{dV}\right) = 0, \tag{22}$$

provides us with an equation which interrelates the derivatives $d\mu/dV$ and $d\bar{\mu}/dV$. Apparently, the regularized expressions for the mean charge of quarks and antiquarks (9) are meant here. Dealing, in a similar way, with the requirement of mean entropy conservation, $d\bar{S}/dV = 0$, we obtain another equation,

$$\int \frac{d\mathbf{p}}{(2\pi)^3}\frac{dn}{d\mu}\ln\frac{n}{1-n}\frac{d\mu}{dV} - \int \frac{d\mathbf{p}}{(2\pi)^3}\frac{d\bar{n}}{d\bar{\mu}}\ln\frac{\bar{n}}{1-\bar{n}}\frac{d\bar{\mu}}{dV} = \frac{\bar{S}}{2N_cV^2}. \tag{23}$$

Substituting here $T\ln(n^{-1} - 1) = -\mu + |P_4|$ and $T\ln(\bar{n}^{-1} - 1) = \bar{\mu} + |P_4|$, we have, after simple calculations taking into account (22), that

$$\int \frac{d\mathbf{p}}{(2\pi)^3}\left(\frac{dn}{d\mu}\frac{d\mu}{dV} + \frac{d\bar{n}}{d\bar{\mu}}\frac{d\bar{\mu}}{dV}\right)|P_4| = -\frac{\bar{S}T}{2N_cV^2} - \frac{\bar{Q}_4\mu}{2N_cV^2}.$$

Eventually, this leads to the following expression for the pressure,

$$P = -\frac{E}{V} + \frac{\bar{S}T}{V} + \frac{\bar{Q}_4\mu}{V} \tag{24}$$

(of course, the thermodynamic potential is $\Omega = -PV$). At small temperatures the antiquark contribution is negligible, and the thermodynamic description can be grounded in utilizing one chemical potential μ only. If the antiquark contribution is getting intrinsic, then the thermodynamic picture becomes more complicated due to the necessity to obey the condition $\bar{\mu} = \mu$ which comes into play. In particular, at zero temperature we might consider the antiquark contribution to be absent and obtain

$$P = -\mathcal{E} + \mu\rho_q,$$

where $\mu = (P_F^2 + M_q^2(P_F))^{1/2}$, P_F is the Fermi momentum, and $\rho_q = N/V$ is the quark ensemble density.

For lucidity of our viewpoint we consider mainly the NJL model [6] in this paper; i.e. the correlation function [the form factor in Eq. (3)] behaves as the δ function in coordinate space. It is a well-known fact that, in order to have an intelligent result in this model, one needs to use a regularization cutting of the momentum integration in Eq. (13). We adjust the standard set of parameters [7] here with $|\mathbf{p}| < \Lambda$, $\Lambda = 631$ MeV, $m = 5.5$ MeV, and $G\Lambda^2/(2\pi^2) = 1.3$. This set at $n = 0$, $\bar{n} = 0$, $T = 0$ gives, for the dynamical quark mass, $M_q = 335$ MeV. In particular, it may be shown that the following representation of the ensemble energy is valid at the extremals of the functional (13),

$$E = E_{\text{vac}} + 2N_cV\int^{\Lambda}\frac{d\mathbf{p}}{(2\pi)^3}|P_4|(n+\bar{n}),$$

$$E_{\text{vac}} = 2N_cV\int^{\Lambda}\frac{d\mathbf{p}}{(2\pi)^3}(|p_4| - |P_4|) + 2N_cV\frac{M^2}{4G}. \tag{25}$$

It is easy to understand that this expression, with the vacuum contribution subtracted, looks like the energy of a gas of relativistic particles and antiparticles with the mass M_q and coincides identically with that calculated in the mean field approximation.

Let us summarize the results of this exercise. So, we determine the density of quark n and antiquark $\bar{n}$ quasiparticles at given parameters μ and T from the second and third equations of system (14). From the first equation we receive the angle of quark and antiquark pairing θ as a function of dynamical quark mass M_q which is handled as a parameter. Then at small temperatures, below 50 MeV, and values of chemical potentials of dynamical quark mass order, $\mu \sim M_q$, there are several branches of solutions for the gap equation. Figure 1 displays the difference of the right and left sides of Eq. (15), which is denoted by Δ at zero temperature, and several values of chemical potential μ(MeV) = 335 (the lowest curve), 340, 350, 360 (the top curve) as a function of the parameter M_q. The zeros of function $\Delta(M_q)$ correspond to the equilibrium values of dynamical quark mass.

The evolution of the chemical potential as a function of charge density $\mathcal{Q}_4 = Q_4/(3V)$ (in units of charge/ fm^3) with the temperature increasing is depicted in Fig. 2 (the factor 3 relates the quark and baryon matter densities). The top curve corresponds to zero temperature. The other curves, from top to bottom, have been calculated for the temperatures $T = 10$ MeV, ..., 50 MeV with spacing $T = 10$ MeV. As it was found in Ref. [5] the chemical potential at zero temperature is first increasing with the charge density increasing, reaches its maximal value, then decreases, and at the densities of order of normal nuclear matter density [8], $\rho_q \sim 0.16/\text{fm}^3$, it becomes almost equal to its vacuum value. Such a behavior of chemical potential results from the fast decrease of dynamical quark mass with the Fermi momentum increasing. It is clear from Fig. 2 that the charge density is still a multivalued function of chemical potential at a temperature slightly below 50 MeV. Figure 3 shows the ensemble pressure P (MeV/fm^3) as a function of charge density $\mathcal{Q}_4$ at several values of temperature. The lowest curve corresponds to zero temperature. The other curves, from bottom to top, correspond to the temperatures $T = 10$ MeV, ..., 50 MeV with spacing $T = 10$ MeV. It is curious to remember now that in Ref. [5] the vacuum pressure estimate for the NJL model was received as 40—50 MeV/fm^3, which is entirely compatible with the results of conventional bag model. Besides, some hints at the presence of an instability (rooted in the anomalous behavior of pressure $dP/dn < 0$;

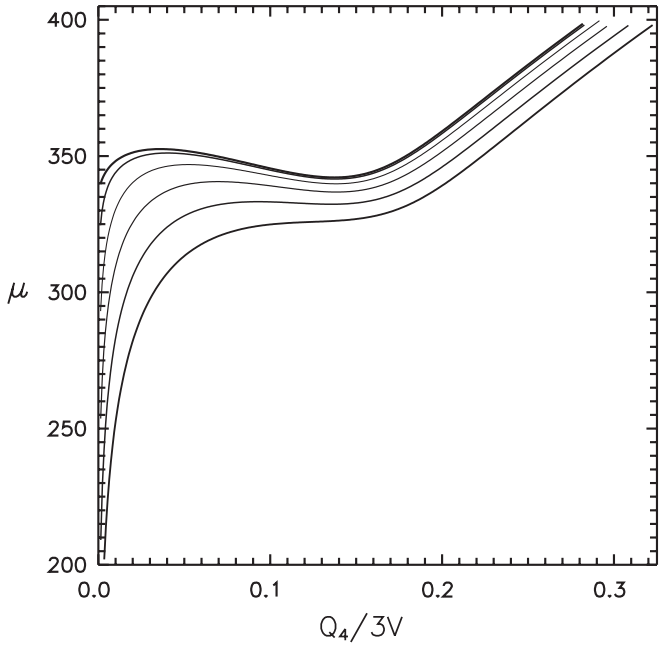

FIG. 2. The chemical potential μ (MeV) is plotted as a function of charge density $\mathcal{Q}_4 = Q_4/(3V)$ (in units of ch/fm^3). The factor 3 relates the densities of quark and baryon matter. The top curve corresponds to the situation of zero temperature. The other curves, from top to bottom, correspond to the temperature values $T = 10$ MeV, ..., 50 MeV with spacing $T = 10$ MeV.

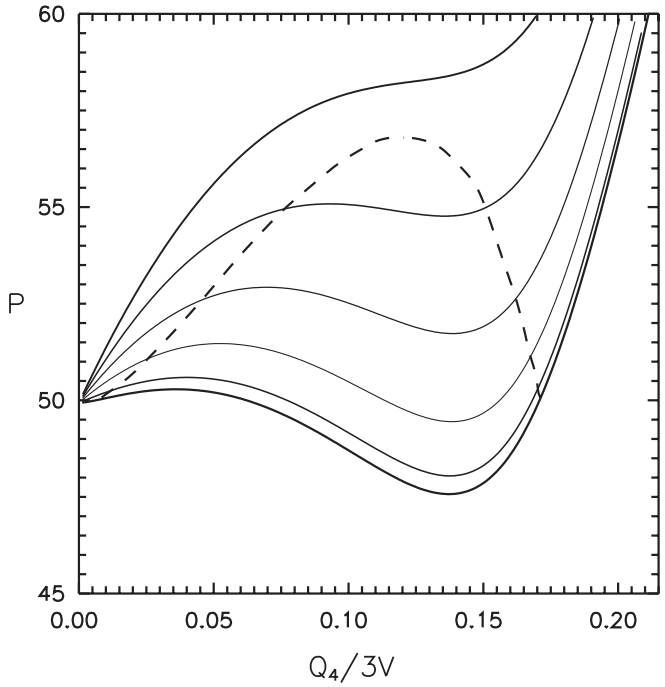

FIG. 3. The ensemble pressure P (MeV/fm^3) is shown as a function of charge density $\mathcal{Q}_4$ at temperatures $T = 0$ MeV, ..., 50 MeV with spacing $T = 10$ MeV. The lowest curve corresponds to zero temperature. The dashed curve shows the boundary of a liquid–gas phase transition; see the text.

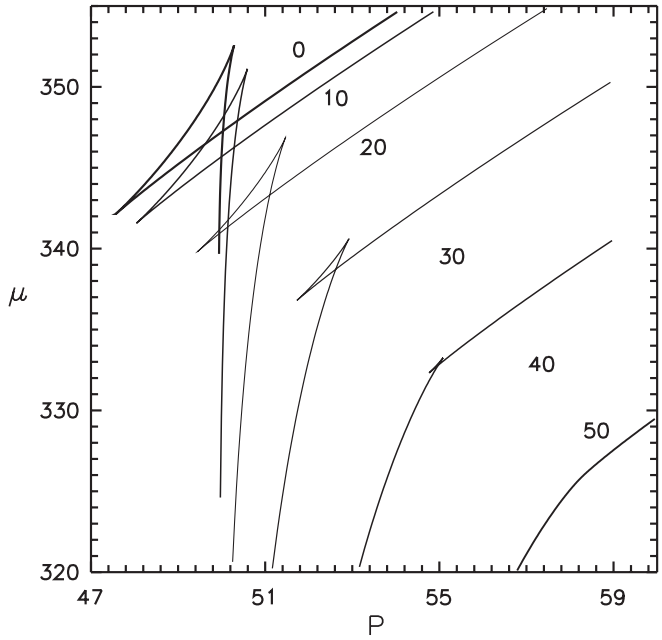

FIG. 4. The fragments of the isotherms in Figs. 2 and 3; see the text. Chemical potential μ (MeV) is plotted as a function of pressure P MeV/fm^3. The top curve corresponds to the zero isotherm, and the other curves following down correspond to the isotherms with spacing of 10 MeV, till the isotherm 50 MeV (the lowest curve).

see also [9,10]) in some interval of the Fermi momentum have been found.

Figure 4 shows the fragments of isotherms of Figs. 2 and 3 but in different coordinates (chemical potential—ensemble pressure). The top curve is calculated at zero temperature; the other isotherms, from top to bottom, correspond to the temperatures increasing with spacing 10 MeV. The lowest curve is calculated at the temperature 50 MeV. This plot obviously demonstrates that there are states on the isotherm which are thermodynamically equilibrated and have equal pressure and chemical potential (see the characteristic Van der Waals triangle with the crossing curves). The equilibrium points calculated are shown in Fig. 3 by the dashed curve. The points of the dashed curve crossing an isotherm pinpoint the boundary of a gas—liquid phase transition. The corresponding straight line $P = \text{const}$ which obeys the Maxwell rule separates the nonequilibrium and unstable fragments of the isotherm and describes a mixed phase. Then the critical temperature for the parameter which we are using in this paper becomes $T_c \sim 45.7$ MeV with the critical charge density $\bar{Q}_4 \sim 0.12$ ch/fm^3. Usually the thermodynamic description is grounded in the mean energy functional, which is the homogeneous function of the particle number, like $E = Nf(S/N, V/N)$ (without a vacuum contribution). It is clear that such a description requires the corresponding subtractions to be introduced; however, this operation does not change the final results considerably. Now, the intuitive arguments of Ref. [5] that the states filled up with quarks and separated from the instability region look like a ''natural construction material'' to form the baryons are getting much more clarity and give a hope to understand the existing fact of equilibrium between the vacuum and octet of stable (in strong interaction) baryons [11].

The dynamical quark mass $|M_q|$ (MeV) as a function of chemical potential μ (MeV) is presented for the temperatures $T = 0\,\text{MeV}, \ldots, 100\,\text{MeV}$ with spacing $T = 10$ MeV in Fig. 5. The rightmost curve corresponds to zero temperature. At small temperatures, below 50 MeV, the dynamical quark mass is the multivalued function of chemical potential. Figure 6 shows the dynamical quark mass as a function of temperature at small values of charge density $\mathcal{Q}_4 \sim 0$. Such a behavior allows us to conclude that the quasiparticle gets larger with increasing temperature. This becomes clear if we remember that the momentum corresponding to the maximal attraction between the quark and antiquark p_θ (according to Ref. [4]) is defined by $d\sin\theta/dp = 0$. In particular, this parameter in the NJL model equals

$$p_\theta = (|M_q|m)^{1/2} \tag{26}$$

but its inverse magnitude defines the characteristic (effective) size of the quasiparticle $r_\theta = p_\theta^{-1}$.

If one is going to define the quark chemical potential as an energy necessary to add (to remove) one quasiparticle

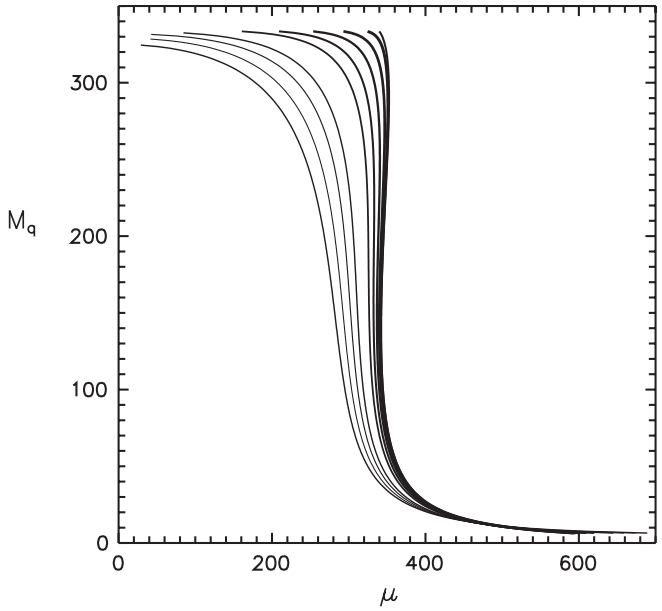

FIG. 5. The dynamical quark mass $|M_q|$ (MeV) is shown as a function of chemical potential μ (MeV) at the temperatures $T = 0$ MeV, ..., 100 MeV with spacing $T = 10$ MeV. The rightmost curve corresponds to zero temperature.

(as it was shown in [5] at zero temperature), $\mu = dE/dN$, then in vacuum (i.e. at quark density ρ_q going to zero) the quark chemical potential magnitude coincides with the quark dynamical mass. It results in the phase diagram displayed at this value of chemical potential, although, in principle, this value could be smaller than the dynamical quark mass, as has been considered in the pioneering paper [12]. If one takes, for example, a chemical potential value

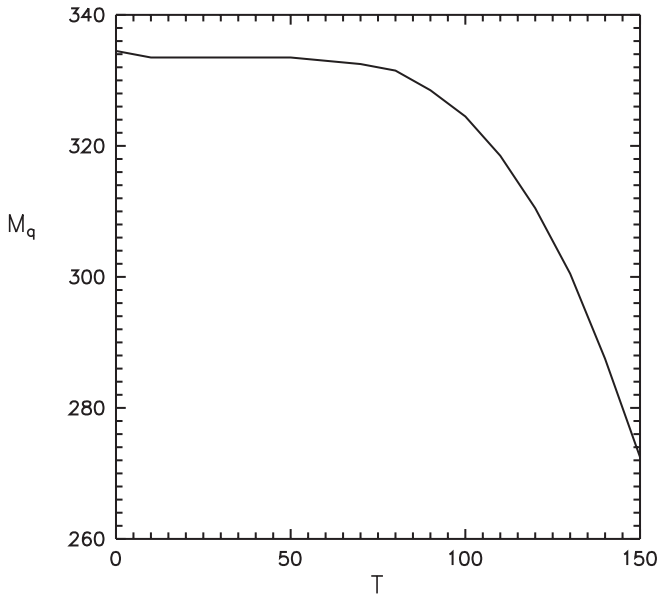

FIG. 6. The dynamical quark mass $|M_q|$ (MeV) as a function of temperature at a small value of charge density $\mathcal{Q}_4$.

of zero, this leads to the conventional picture, but, obviously, such a configuration does not correspond to the real process of filling up the Fermi sphere with quarks.

Apparently, our study of the quark ensemble thermodynamics produces quite reasonable arguments to propound the hypothesis that the phase transition of chiral symmetry (partial) restoration has already been realized as the mixed phase of the physical vacuum and baryonic matter [13]. However, it is clear that our quantitative estimates should not be taken as appropriate for comparing with, for example, the critical temperature of the nuclear matter phase transition which has been experimentally measured and is equal to 15–20 MeV. Besides, the gas component (at $T = 0$) has nonzero density (0.01 of the normal nuclear density) but in reality this branch should correspond to the physical vacuum, i.e. zero baryonic density [15]. In principle, the idea of global equilibrium of gas and liquid phases prompted us to put down adequate boundary conditions to describe the transitional layer existing between the vacuum and the filled-up state and to calculate the surface tension effects. It seems plausible that the changes taking place in this layer could ascertain all ensemble processes similar to the theory of Fermi liquids.

III. TRANSITION LAYER BETWEEN GAS AND LIQUID

The concept advanced would obtain the substantial confirmation if we are able to demonstrate an existence of a transition layer at which the ensemble transformation from one aggregate state to another takes place. As it was argued above, the indicative characteristic to explore a homogeneous phase (at finite temperature) is the mean charge (density) of ensemble. It was demonstrated that the other characteristics, for example, a chiral condensate, a dynamical quark mass, etc., could be reconstructed as well. So, here we are analyzing the transition layer at zero temperature.

If one assumes the parameters of the gas phase are approximately the same as those at zero charge $\rho_g = 0$, i.e. as in vacuum (this means ignoring the negligible distinctions in the pressure, chemical potential, and quark condensate), the dynamical quark mass develops the maximal value, and for the parameter choice of the NJL model, it is $M = 335$ MeV. Then from the Van der Waals diagram one may conclude that the liquid phase being in equilibrium with the gas phase develops the density $\rho_l = 3 \times 0.185$ ch/fm^3 (for some reason which becomes clear below, we correct it in favor of the value $\rho_l = 3 \times 0.157$ ch/fm^3). The detached factor 3 here links, again, the magnitudes of the quark and baryon densities. The quark mass is approximately $\overset{*}{M} \approx 70$ MeV in this phase (and we are dealing with the simple one-dimensional picture hereafter).

The precursor experience teaches us that an adequate description of heterogeneous states can be reached with

the mean field approximation [16]. In our particular case this means making use of the corresponding effective quark-meson Lagrangian [17] (the functional of Ginzburg-Landau type)

$$\mathcal{L} = -\bar{q}(\hat{\partial} + M)q - \frac{1}{2}(\partial_\mu \sigma)^2 - U(\sigma) - \frac{1}{4}F_{\mu\nu}F_{\mu\nu} - \frac{m_v^2}{2}V_\mu V_\mu - g_\sigma \bar{q}q\sigma + ig_v \bar{q}\gamma_\mu q V_\mu, \tag{27}$$

where

$$F_{\mu\nu} = \partial_\mu V_\nu - \partial_\nu V_\mu, \qquad U(\sigma) = \frac{m_\sigma^2}{2}\sigma^2 + \frac{b}{3}\sigma^3 + \frac{c}{4}\sigma^4,$$

σ is the scalar field, V_μ is the field of vector mesons, m_σ, m_v are the masses of scalar and vector mesons, and g_σ, g_v are the coupling constants of the quark-meson interaction. The $U(\sigma)$ potential includes the nonlinear terms of sigma-field interactions up to the fourth order. For the sake of simplicity we do not include the contribution coming from the pseudoscalar and axial-vector mesons.

The meson component of such a Lagrangian should be self-consistently treated by considering the corresponding quark loops. [In terms of a relativistic extension of the Landau theory of a Fermi liquid, the density fluctuations (meson field collective modes) are nothing more than zero sound, as was shown in Ref. [10]]. Here we do not see any reason to go beyond the well-elaborated and reliable one loop approximation (27) [17], although recently considerable progress has been reached (as we mentioned at the beginning of this paper) in scrutinizing the nonhomogeneous quark condensates by the application of powerful methods of exact integration [18]. Here we believe it is more practical to phenomenologically adjust the effective Lagrangian parameters based on the transparent physical picture. It is easy to see that, handling (27) in the one loop approximation, we come, in actual fact, to the Walecka model [19] but adopted for the quarks. In what follows we work with the designations of that model and hope this does not lead to misunderstandings.

In the context of our paper we propose to interpret Eq. (27) in the following way. Each phase might be considered, in a sense, with regard to another phase as an excited state which requires an additional (apart from a charge density) set of parameters (for example, the meson fields) for its complete description, and those characterize the measure of deviation from the equilibrium state. Then the crucial question becomes whether it is possible to adjust the parameters of effective Lagrangian (27) to obtain the solutions in which the quark field interpolates between the quasiparticles in the gas (vacuum) phase and the quasiparticles of the filled-up states. The density of the filled-up state ensemble should asymptotically approach the equilibrium value of ρ_l and should turn to the zero value in the gas phase (vacuum).

The scale inherent in this problem may be assigned to one of the masses referred to in the Lagrangian (27). In particular, we bear in mind the dynamical quark mass in the vacuum M. Besides, there are four other independent parameters in the problem, and in order to compare them with the results of studying nuclear matter, we employ the form characteristic for the (nuclear) Walecka model,

$$C_s = g_\sigma \frac{M}{m_\sigma}, \qquad C_v = g_v \frac{M}{m_v}, \qquad \bar{b} = \frac{b}{g_\sigma^3 M}, \qquad \bar{c} = \frac{c}{g_\sigma^4}.$$

Taking the parametrization of the potential $U(\sigma)$ as $b_\sigma = 1.5 m_\sigma^2 (g_\sigma/M)$, $c_\sigma = 0.5 m_\sigma^2 (g_\sigma/M)^2$, we come to the sigma model, but the choice $b = 0$, $c = 0$ results in the Walecka model. As to the standard nuclear matter application the parameters b and c demonstrate a vital model-dependent character and are quite different from the parameter values of the sigma model. Truly, in that case their values are also regulated by the additional requirement of an accurate description of the saturation property. On the other hand, for the quark Lagrangian (27) we could intuitively anticipate some resemblance with the sigma model and, hence, could introduce two dimensionless parameters η and ζ in the forms $b = \eta b_\sigma$, $c = \zeta^2 c_\sigma$ which characterize some fluctuations of the effective potential. Then the scalar field potential is presented as follows:

$$U(\sigma) = \frac{m_\sigma^2}{8}\frac{g_\sigma^2}{M^2}\left(4\frac{M^2}{g_\sigma^2} + 4\frac{M}{g_\sigma}\eta\sigma + \zeta^2\sigma^2\right)\sigma^2.$$

The meson and quark fields are defined by the following system of the stationary equations:

$$\begin{aligned} &\Delta\sigma - m_\sigma^2\sigma = b\sigma^2 + c\sigma^3 + g_\sigma \rho_s, \\ &\Delta V - m_v^2 V = -g_v \rho, \\ &(\hat{\nabla} + \overset{*}{M})q = (E - g_v V)q, \end{aligned} \tag{28}$$

where $\overset{*}{M} = M + g_\sigma\sigma$ is the running value of the dynamical quark mass, E stands for the quark energy, and $V = -iV_4$. The density matrix describing the quark ensemble at $T = 0$ has the form

$$\xi(x) = \int^{P_F} \frac{d\mathbf{p}}{(2\pi)^3} q_{\mathbf{p}}(x)\bar{q}_{\mathbf{p}}(x),$$

in which $\mathbf{p}$ is the quasiparticle momentum and the Fermi momentum P_F is defined by the corresponding chemical potential. The densities ρ_s and ρ on the right-hand sides of Eq. (28) are, by definition,

$$\rho_s(x) = \mathrm{Tr}\{\xi(x), 1\}, \qquad \rho(x) = \mathrm{Tr}\{\xi(x), \gamma_4\}.$$

Here we confine ourselves to the Thomas-Fermi approximation while describing the quark ensemble. Then the densities which we are interested in are given, with some local Fermi momentum $P_F(x)$, as

$$\rho = \gamma \int^{P_F} \frac{d\mathbf{p}}{(2\pi)^3} = \frac{\gamma}{6\pi^2} P_F^3,$$

$$\rho_s = \gamma \int^{P_F} \frac{d\mathbf{p}}{(2\pi)^3} \frac{\overset{*}{M}}{E} = \frac{\gamma}{4\pi^2} \overset{*}{M} P_F^2 \left\{ (1+\lambda^2)^{1/2} - \frac{\lambda^2}{2} \ln\left[\frac{(1+\lambda^2)^{1/2}+1}{(1+\lambda^2)^{1/2}-1} \right] \right\}, \tag{29}$$

where γ is the quark factor which, for one flavor, is $\gamma = 2N_c$ (N_c is the number of colors), $E = (\mathbf{p}^2 + \overset{*}{M}{}^2)^{1/2}$, and $\lambda = \overset{*}{M}/P_F$. By definition, the ensemble chemical potential does not change, and it leads to the situation in which the local value of the Fermi momentum is defined by the running value of the dynamical quark mass and vector field as

$$\mu = M = g_v V + (P_F^2 + \overset{*}{M}{}^2)^{1/2}. \tag{30}$$

Now we should tune the Lagrangian parameters (27). For asymptotically large distances (in the homogeneous phase) we may neglect the gradients of scalar and vector fields, and the equation for the scalar field in the system (28) leads to the first equation which bounds the parameters C_s, C_v, $\bar{b}$, $\bar{c}$:

$$\frac{M^2(\overset{*}{M} - M)}{C_s^2} + \bar{b} M (\overset{*}{M} - M)^2 + \bar{c} (\overset{*}{M} - M)^3 = -\rho_s. \tag{31}$$

The asymptotic vector field is given by the ensemble density $V = C_v^2 \rho/(g_v M^2)$. The second equation results from the relation (30) for the chemical potential and gives

$$M = \frac{C_v^2 \rho}{M^2} + (P_F^2 + \overset{*}{M}{}^2)^{1/2}. \tag{32}$$

Extracting the liquid density from (29), we obtain the Fermi momentum ($P_F = 346$ MeV). Applying the identities (31) and (32), we have for the particular case $b = 0$, $c = 0$ that $C_s^2 = 25.3$, $C_v^2 = -0.471$; i.e. the vector component C_v^2 is small (compared to C_s^2) and has negative value which is unacceptable. Apparently, it seems necessary to neglect the contribution coming from the vector field or to diminish the dynamical quark mass $\overset{*}{M}$ up to the value which retains the identity (32) valid with positive C_v^2 or equal to zero. In the gas phase the dynamical quark mass can also be corrected to a value larger than the vacuum value. It is clear that in the situation of the liquid with the density $\rho_l = 3 \times 0.185$ ch/fm^3, the dynamical quark mass should coincide with (or exceed) $M = 346$ MeV in the gas phase. However, here we correct the liquid density (as it was argued above) to decrease its value up to $\rho_l = 3 \times 0.157$ ch/fm^3, which is quite acceptable in the capacity of normal nuclear matter density. In fact, this possibility can be simply justified by another choice of the NJL model parameters. Thus, we obtain at $\overset{*}{M} = 70$ MeV and $b = 0$, $c = 0$ that $C_s^2 = 28.4$, $C_v^2 = 0.015$; i.e. we have a small but positive value for the vector field coefficient. At the same time, aiming here to estimate the surface tension effects only, we do not strive for the precise fit of parameters. In the Walecka model these coefficients are $C_s^2 = 266.9$, $C_v^2 = 145.7$ ($b = 0$, $c = 0$). Moreover, there is another parameter set with $C_s^2 = 64$, $C_v^2 \approx 0$ [20], but it is rooted in an essential nonlinearity of the sigma field due to the nontrivial values of the coefficients b and c. The option (formally unstable) with negative c (b) has also been discussed.

The coupling constant of the scalar field is fixed by the standard (for the NJL model) relation between the quark mass and the π-meson decay constant $g_\sigma = M/f_\pi$ (we put $f_\pi = 100$ eV), although there is no objection to treating this coupling constant as an independent parameter. As a result of all the agreements done, we have, for the σ-meson mass, $m_\sigma = g_\sigma M/C_s$. In principle, we could even fix the σ-meson mass and coupling constant g_σ, but all the relations mentioned above eventually lead to quite suitable values of the σ-meson mass, as will be demonstrated below.

The vector field plays, as we will see, a secondary role because of the small magnitude of constant C_v. Then, taking the vector meson mass as $m_v \approx 740$ MeV (slightly smaller than the mass of the ω meson for simple technical reasons only) we calculate the coupling constant of the vector field from a relation similar to the scalar field $m_v = g_v M/C_v$. Amazingly, its value is steadily small compared to the value characteristic for the NJL model, $g_v = \sqrt{6} g_\sigma$. However, at the values of constant C_v which we are interested in, it is very difficult to maintain reasonable balance, and for the sake of clarity, we prefer to choose the massive vector field. Actually, this is unessential because we need this parameter (as we remember) only to estimate the vector field strength.

The key point of our interest here is the surface tension coefficient [20] which can be defined as

$$u_s = 4\pi r_o^2 \int_{-\infty}^{\infty} dx \left[\mathcal{E}(x) - \frac{\mathcal{E}_l}{\rho_l} \rho(x) \right]. \tag{33}$$

The parameter r_o will be discussed in the next section by considering the features of a quark liquid droplet, and for now we would like to note only that, for the parameters considered, its magnitude for $N_f = 1$ is around $r_o = 0.79$ fm. Recalling the factor $3^{1/3}$ which connects the baryon and quark numbers, one can find that the magnitude ($\tilde{r}_o = 3^{1/3} 0.79 \approx 1.14$ fm) is in full agreement with the magnitude standard for the nuclear matter calculations (in the Walecka model) $\tilde{r}_o = 1.1$—1.3 fm.

In order to proceed we calculate $\mathcal{E}(x)$ in the Thomas-Fermi approximation as

$$\mathcal{E}(x) = \gamma \int^{P_F(x)} \frac{d\mathbf{p}}{(2\pi)^3} [\mathbf{p}^2 + \overset{*}{M}(x)]^{1/2} + \frac{1}{2} g_v \rho(x) V(x) - \frac{1}{2} g_\sigma \rho_s(x) \sigma(x).$$

And to give some idea for the "setup" prepared, we present here the characteristic parameter values for some fixed b and c with $\rho_l = 3 \times 0.157$ ch/fm^3. In the liquid phase they are $\overset{*}{M} = 70$ MeV ($P_F = 327$ MeV) and $e_l = 310.5$ MeV [the index l stands for a liquid phase and $e(x) = \mathcal{E}(x)/\rho(x)$ defines the density of specific energy]. Both Eqs. (31) and (32) are obeyed by this state. There exists the solution with a larger value of the quark mass, $\overset{*}{M} = 306$ MeV ($P_F = 135$ MeV) (we have faced a similar situation in the first section, dealing with the gas of quark quasiparticles), and $e = 338$ MeV $\sim e_g$ (e_g is the specific energy in the gas phase), which satisfies both equations as well. The specific energy of this solution appears to be larger than the specific energy of the previous solution. It is worthwhile to mention the existence of an intermediate state corresponding to the saturation point with the mass $\overset{*}{M} = 95$ MeV ($P_F = 291$ MeV) and $e = 306$ MeV. Obviously, it is the most favorable state with the smallest value of specific energy (and with zero pressure of the quark ensemble), and the system can reach this state only in the presence of a significant vector field. This state (already discussed in the first section) corresponds to the minimal value of the chemical potential ($T = 0$) and can be reached at the densities typical for normal nuclear matter. However, Eq. (32) is not valid for this state.

Two other parameters η, ζ are fixed by looking through all the configurations in which the solution of equation system (28) with a stable kink in the scalar field does exist and describes the transition of the gas phase quarks to the liquid phase. First, it is reasonable to scan the η, c ($\zeta = c\eta$) plane, in order to identify the domain in which the increase of specific energy $\mathcal{E} - \mathcal{E}_l \rho/\rho_l \leq 0$ is revealed by running through all possible states which provide the necessary transition (without taking into account the field gradients). In practice, one needs to follow a simple heuristic rule. The state with $P_F \sim 1$ MeV (i.e. e and the corresponding ρ) and the state of characteristic liquid energy $\mathcal{E}_l$ (together with ρ_l) should be compared at scanning the Lagrangian parameters η and c. Just this domain where they are commensurable could provide us with the solutions in which we are interested, and Fig. 7 shows its boundary. The curve could be continued beyond the value $\eta = 2.5$, but the values of the corresponding parameter η are unrealistic and not shown in the plot.

We calculate the solution of equation system (28) numerically by the Runge-Kutta method with the initial conditions $\sigma(L) \approx 0$, $\sigma'(L) \approx 0$ imposed at large distances $L \gg t$, where t is a characteristic thickness of the transition layer (about 2 fm). Such a simple algorithm appears to be quite suitable if the vector field contribution is considered as a small correction (which just takes place in the situation under consideration) and is presented as

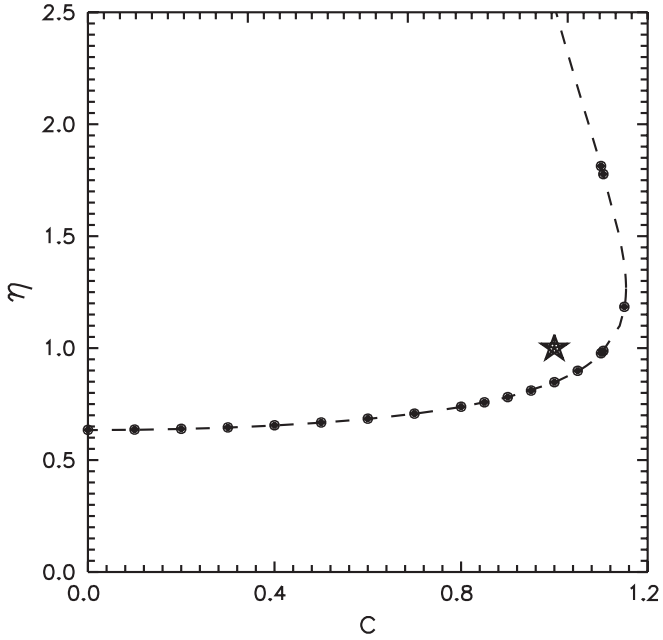

FIG. 7. The domain of the η, c ($\zeta = c\eta$) plane in which an increase of specific energy occurs; see the text. The dots represent a stable kink. The star shows the position of the canonical (chiral) kink; see the text.

$$V(x) = \frac{1}{2m_v} \int_{-L}^{L} dz e^{-m_v|x-z|} g_v \rho(z),$$

where the charge (density) ρ is directly defined by the scalar field. We considered the solutions including the contribution of the vector field, and the corresponding results confirm the estimates obtained.

A rather simple analysis shows that the interesting solutions are located along the boundary of the discussed domain. Some of those are depicted in Fig. 7 as dots. Figure 8 shows the stable kinks of the σ field with the parameter $c = 1.1$ for two existing solutions with $\eta \approx 0.977$ ($m_\sigma \approx 468$ MeV) (solid line) and $\eta \approx 1.813$ ($m_\sigma \approx 690$ MeV) (dashed line). For the sake of clarity, we consider that the gas (vacuum) phase is on the right. Then the asymptotic value of the σ field on the left-hand side ($\sigma \approx 80$ MeV) corresponds to $\overset{*}{M} = 70$ MeV. The thickness of the transition layer for the solution with $\eta \approx 0.977$ is $t \approx 2$ fm, while for the second solution $t \approx 1$ fm.

Characterizing the whole spectrum of solutions obtained, we should mention that there exist other more rigid (chiral) kinks which correspond to the transition into the state with the dynamical quark mass changing its sign, i.e. $M \rightarrow -M$. In particular, the kink with the canonical parameter values $\eta = 1$, $c = 1$ is clearly seen (marked by the star in Fig. 7), and its surface tension coefficient is about

$2m_\pi$ (m_π is the π-meson mass). The most populated class of solutions consists of those having metastable character. The system comes back to the starting point (after an evolution) pretty rapidly, and usually the σ field does not evolve to such an extent that it reaches the asymptotic value (which corresponds to the dynamical quark mass in the liquid phase $\overset{*}{M} = 70$ MeV). Switching on the vector field changes the solutions insignificantly (for our situation with small C_v, it does not exceed 2 MeV).

The surface tension coefficient u_s in MeV for the curve of stable kinks with the parameter $\eta \leq 1.2$ as a function of the parameter c ($\zeta = c\eta$) is depicted in Fig. 9. The σ-meson mass at $c \approx 0$ is $m_\sigma \approx 420$ MeV and changes smoothly up to the value $m_\sigma \approx 500$ MeV at $c \approx 1.16$ (the maximal value of the coefficient c beyond which the stable kink solutions are not observed). In particular, $m_\sigma \approx 450$ MeV at $c = 1$. Two kink solutions with $c = 1.1$ for $\eta \approx 0.977$ and for $\eta \approx 1.813$ (both are shown in Fig. 8, and only the first one is shown in Fig. 9) have the tension coefficient values $u_s \approx 35$ MeV and $u_s \approx 65$ MeV, correspondingly. The maximal value of the tension coefficient for normal nuclear matter does not exceed $u_s = 50$ MeV. The nuclear Walecka model claims the value $u_s \approx 19$ MeV [20] as acceptable and calculable. The reason for this higher value of surface tension coefficient for quarks is rooted in the different magnitudes of the mass deficit. Indeed, for nuclear matter it does not exceed $\overset{*}{M} \approx 0.5M$, albeit more realistic values are considered around $\overset{*}{M} \approx 0.7M$, and for the quark ensemble the mass deficit amounts to $\overset{*}{M} \approx 0.3M$. We are also able to estimate the compression coefficient of quark matter K which appears significantly larger than the nuclear one. Actually, we see quite a smooth analogy between the results of Sec. III and the results of the bag soliton model [21]. The thermodynamic treatment developed in the present paper allows us to formulate adequate boundary conditions for the bag in a physical vacuum and to diminish considerably the uncertainties in searching the true soliton Lagrangian. We believe it was also shown here that to single out one soliton solution among others (including even those obtained by the exact integration method [18]), which describes the transitional layer between two media, is not an easy problem if the boundary conditions formulated above are not properly imposed.

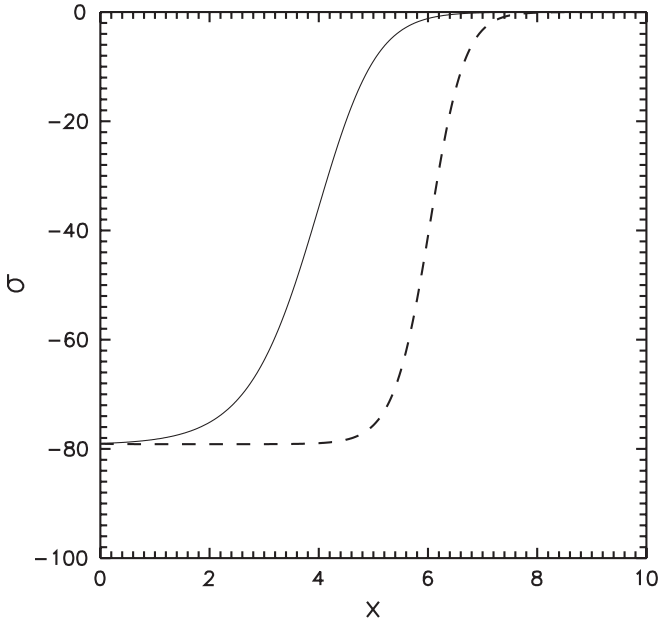

FIG. 8. The stable kink solutions with $c = 1.1$. The solid line corresponds to $\eta \approx 0.977$ ($m_\sigma \approx 468$ MeV), and the dashed line corresponds to $\eta \approx 1.813$ ($m_\sigma \approx 690$ MeV). x is given in units of fm and σ is given in MeV.

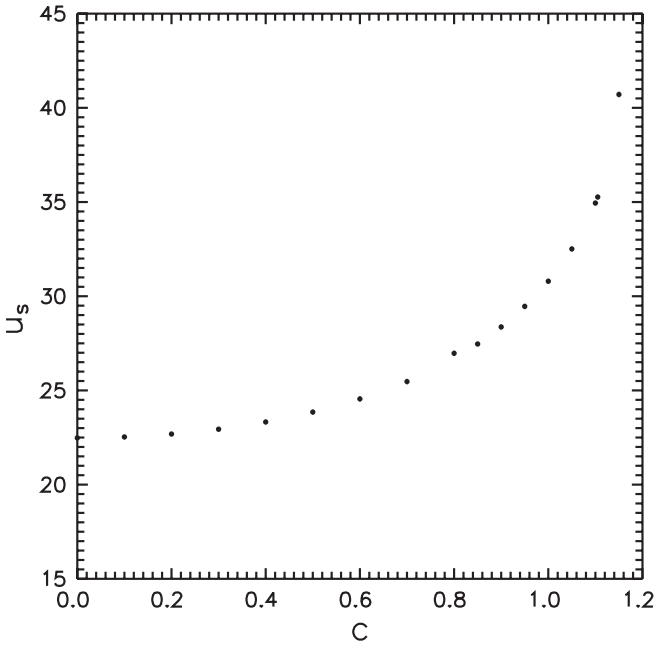

FIG. 9. The surface tension coefficient u_s in MeV as a function of the parameter c ($\zeta = c\eta$) for the curve of stable kinks (with $\eta \leq 1.2$).

IV. DROPLET OF QUARK LIQUID

The results of the two previous sections have led us to pose the challenging question about the creation and properties of finite quark systems or the droplets of quark liquid which are in equilibrium with the vacuum state. Thus, as a droplet we imply the spherically symmetric solution of the equation system (28) for $\sigma(r)$ and $V(r)$ with the obvious boundary conditions $\sigma'(0) = 0$ and $V'(0) = 0$ in the origin (the primed variables denote the first derivatives in r), rapidly decreasing at the large distances $\sigma \to 0$, $V \to 0$, when $r \to \infty$.

A quantitative analysis of similar nuclear physics models which includes the detailed tuning of parameters is usually based on the comprehensive fitting of available

experimental data. This is obviously irrelevant in studying the quark liquid droplets. This global difficulty dictates specific tactics for analyzing. We propose to start, first of all, by selecting the parameters which could be worthwhile to play the role of physical observables. Naturally, the total baryon number which is phenomenologically (via a factor 3) related to the number of valence quarks in an ensemble is a reasonable candidate for this role. Besides, the density of the quark ensemble $\rho(r)$, the mean size of droplet R_0, and the thickness of surface layer t seem suitable for such an analysis.

It is argued above that the vector field contribution is negligible because of the smallness of the coefficient C_v compared to the C_s magnitude, and we follow this conclusion (or assumption), albeit it is scarcely justified in the context of a finite quark system. Thus, we will put $g_v = 0$, $V = 0$ in what follows, and it will simplify all the calculations enormously.

Figure 10 shows the set of solutions (σ field in MeV) of the system (28) at $N_f = 1$, and Fig. 11 presents the corresponding distributions of the ensemble density ρ (ch/fm^3). The parameters C_s, C_v, b, and c are derived by the same algorithm as in the previous section; i.e. the chemical potential of the quark ensemble $M = 335$ (and $\sigma \to 0$) is fixed at spatial infinity. The filled-up states (liquid) are characterized by the parameters $\overset{*}{M} = 70$ MeV, $\rho_0 = \rho_l = 3 \times 0.157$ ch/fm^3. The σ-meson mass and the coupling constant g_σ are derived at fixed coefficients η and ζ, and they just define the behavior of solutions $\sigma(r)$, $\rho(r)$, etc. The magnitudes of the functions $\sigma(r)$ and $\rho(r)$ at the origin

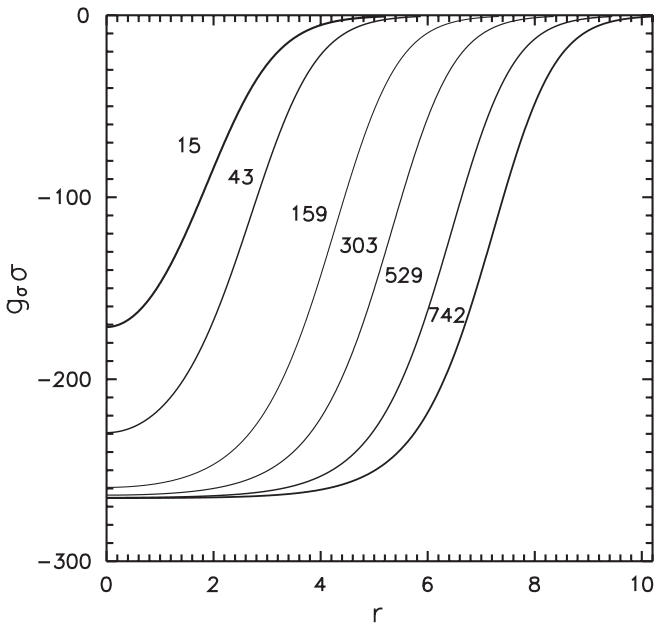

FIG. 10. The σ field (MeV) as a function of the distance r (fm) for several solutions of the equation system (28) which are characterized by the net quark number N_q written to the left of each curve.

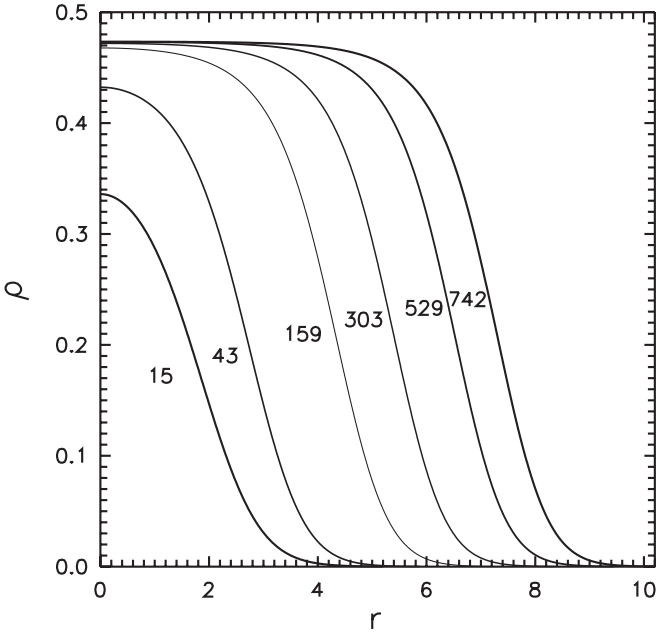

FIG. 11. Distribution of the quark density ρ (ch/fm^3) for the corresponding solutions presented in Fig. 11.

are not strongly correlated with the values characteristic of the filled-up states and are practically determined by solving the boundary value problem for system (28). In particular, the solutions presented in Fig. 10 have been obtained with the running coefficient η at $\zeta = \eta$. The most relevant parameter (instead of η) from the physical viewpoint is the total number of quarks in the droplet N_q (as discussed above), and it is depicted to the left of each curve. (The variation of $\overset{*}{M}$, ρ_0, and f_π could be considered as well instead of the two mentioned parameters η and ζ.)

Analyzing the full spectrum of solutions obtained by scanning one can reveal a recurrent picture (at a certain scale) of kink droplets which are easily parametrized by the total number of quarks N_q in a droplet and by the density ρ_0. These characteristics are evidently fixed when completing the calculations. The sign which allows us to single out these solutions is related to the value of the droplet's specific energy (see below).

Table I exhibits the results of fitting the density $\rho(r)$ with the Fermi distribution,

$$\rho_F(r) = \frac{\tilde{\rho}_0}{1 + e^{(R_0 - r)/b}}, \tag{34}$$

where $\tilde{\rho}_0$ is the density at the origin, R_0 is the mean size of the droplet, and the parameter b defines the thickness of the surface layer $t = 4\ \ln(3)b$. Besides, the coefficient r_0 which is absorbed in the surface tension coefficient (33), the σ-meson mass, $R_0 = r_0 N_q^{1/3}$, and the coefficient η at which all other values have been obtained are also presented in Table I.

The curves plotted in Fig. 10 and the results of Table I allow us to conclude that the density distributions at

TABLE I. Results of fitting by the Fermi distribution with $N_f = 1$, $\tilde{\rho}_0$ (ch/fm^3), R_0, t, r_0, b (fm), m_σ (MeV).

N_q	$\tilde{\rho}_0$	R_0	b	t	r_0	m_σ	η
15	0.34	1.84	0.51	2.24	0.74	351	0.65
43	0.43	2.19	0.52	2.28	0.75	384	0.73
159	0.46	4.19	0.52	2.29	0.77	409	0.78
303	0.47	5.23	0.52	2.29	0.78	417	0.795
529	0.47	6.37	0.52	2.27	0.79	423	0.805
742	0.47	7.15	0.52	2.27	0.79	426	0.81

TABLE II. Results of fitting by the Fermi distribution with $N_f = 2$, $\tilde{\rho}_0$ (ch/fm^3), R_0, t, r_0, b (fm), m_σ (MeV).

N_q	$\tilde{\rho}_0$	R_0	b	t	r_0	m_σ	η
18	0.81	1.56	0.67	1.63	0.57	524	0.7
46	0.9	2.14	0.37	1.63	0.6	557	0.75
169	0.93	3.43	0.36	1.6	0.62	586	0.79
278	0.94	4.08	0.36	1.6	0.62	594	0.8
525	0.94	5.04	0.36	1.6	0.62	603	0.81
776	0.94	5.76	0.36	1.6	0.63	607	0.815

$N_q \geq 50$ are in full agreement with the corresponding data typical for nuclear matter. The thicknesses of the transition layers in both cases are also similar, and the coefficient r_0 with the factor $3^{1/3}$ included is in full correspondence with $\tilde{r}_0$. The values of the σ-meson mass in Table I look quite reasonable as well. However, the corresponding quantities are very different at small quark numbers in the droplet. We know from the experiments that in nuclear matter some increase of the nuclear density is observed. It becomes quite considerable for helium and is much larger than the standard nuclear density for hydrogen.

Obviously, we understand that the Thomas-Fermi approximation which is used for estimating becomes hardly justified at a small number of quarks, and we should deal with the solutions of the complete equation system (28). However, one very encouraging hint comes from the chiral soliton model of the nucleon [22], where it has been demonstrated that by solving this system (28) a good description of the nucleon and Δ can be obtained. Then our original remark could be that the soliton solutions obtained in [22] permit an interpretation as a confluence of two kinks. Each of those kinks ''works'' on the restoration of chiral symmetry since the scalar field approaches its zero value at a distance of $\sim$0.5 fm from the kink center. Indeed, one branch of our solution corresponds to a positive value of the dynamical quark mass, and another branch presents the solution with negative dynamical quark mass (in the three-dimensional picture the pseudoscalar fields appear just as a phase of chiral rotation from a positive to a negative value of the quark mass). Such solutions develop the surface tension coefficient which is larger by a factor 2 than the corresponding coefficient of a single kink, and we believe they signal some instability of a single kink solution.

Similar results are obtained for two flavors $N_f = 2$ ($\gamma = 2N_f N_c = 12$), assuming that all dynamical quark masses of the SU(2) flavor multiplet are equal. The solutions for the σ field and density distributions are similar to the corresponding results presented in Figs. 10 and 11. The other data of fitting solutions are shown in Table II. As it is seen, the characteristic ensemble density is approximately a factor 2 larger than the density of normal nuclear matter (remember again the factor 3). The characteristic values of the σ-meson mass are slightly larger than for $N_f = 1$ and, consequently, the thickness of the transition layer is smaller almost by a factor 1.4. The coefficient interrelating the mean size of the droplet and the baryon (quark) number $\tilde{r}_0 \sim 0.8$ is getting smaller. In principle, one can correct (increase) the surface layer thickness and the parameter $\tilde{r}_0$ by decreasing the σ-meson mass, but the ensemble density remains higher than the normal nuclear one.

Figure 12 displays the specific binding energy of the ensemble. It is defined by an expression similar to Eq. (33) in which the integration over the quark droplet volume is performed. The specific energy is normalized (compared) to the ensemble energy at spatial infinity, i.e. in vacuum. Actually, Fig. 12 shows several curves in the upper part of the plot which correspond to the calculations with $N_f = 1$. The solid line is obtained by scanning over the parameter η and corresponds to the data presented in Table I. The dashed curve is calculated at fixed $\eta = 0.4$ but by scanning over the parameter $\overset{*}{M}$. It is clearly seen that, if the specific energy data are presented as a function of quark number N_q, then the solutions in which we are interested rally in

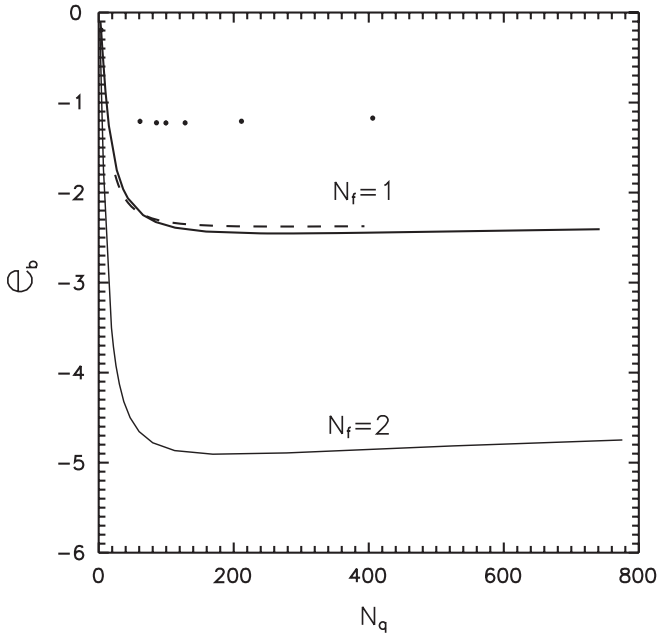

FIG. 12. The specific binding energy at $N_f = 1$ and $N_f = 2$ in MeV as a function of quark number N_q.

the local vicinity of the curve where the maximal binding energy $|\mathcal{E}_b|$ is reached.

A similar solution scanning can be performed over the central density parameter ρ_0 at the origin. The corresponding data are dotted for a certain fixed $\overset{*}{M}$ and ρ_0. It is interesting to notice that, by scanning over any variable discussed, a saturation property is observed, and it looks like the minimum in e_b at $N_q \sim 200$–250. The results for the specific binding energy as a function of particle number are in qualitative agreement with the corresponding experimental data. And one may even say this about the quantitative agreement if the factor 3 (the energy necessary to remove one baryon) is taken into account. Another interesting fact to mention is that there exist solutions of system (28) with positive specific energy. For example, for $N_f = 2$ such metastable solutions appear at sufficiently large η and with the density parameter at the origin equal to $\rho_0 \sim \rho_l = 0.157$ ch/fm^3. In fact, the equation system (28) represents an equation of balance for the current quarks circulating between liquid and gas phases.

As a conclusion, we would like to emphasize that, in the present paper, we have demonstrated how a phase transition of the liquid–gas kind (with reasonable values of parameters) emerges in the NJL-type models. The constructed quark ensemble displays some interesting features for the nuclear ground state (for example, an existence of the state degenerate with the vacuum one), and the results of our study are suggestive to speculate that the quark droplets could coexist in equilibrium with the vacuum under normal conditions. These droplets manifest themselves as bearing a strong resemblance to the nuclear matter. Elaborating this idea in detail is a great challenge which will take a lot of special effort, and we do hope to undertake this challenge in the near future.

ACKNOWLEDGMENTS

The authors are deeply indebted to K. A. Bugaev, R. N. Faustov, S. B. Gerasimov, E.-M. Ilgenfritz, K. G. Klimenko, E. A. Kuraev, A. V. Leonidov, V. A. Petrov, A. M. Snigirev, and many other colleagues for numerous fruitful discussions.

APPENDIX A: MEAN ENERGY FUNCTIONAL

The free part of the Hamiltonian,

$$H_0 = -\int d\mathbf{x}\bar{q}(\mathbf{x})(i\boldsymbol{\gamma}\boldsymbol{\nabla} + im)q(\mathbf{x})$$
$$= \int \frac{d\mathbf{p}}{(2\pi)^3}|p_4|[\cos\theta(A^+(\mathbf{p};s)A(\mathbf{p};s) - B(\mathbf{p};s)B^+(\mathbf{p};s)) + \sin\theta(A^+(-\mathbf{p};s)B^+(\mathbf{p};s) + B(-\mathbf{p};s)A(\mathbf{p};s))],$$

contributes to the mean energy as

$$\mathrm{Tr}\{\xi\mathcal{H}_0\} = \int \frac{d\mathbf{p}}{(2\pi)^3}|p_4|(1-\cos\theta) + \int \frac{d\mathbf{p}}{(2\pi)^3}|p_4|\cos\theta[n(p)+\bar{n}(p)], \quad \text{(A1)}$$

where $\mathcal{H}_0 = H_0/(V2N_c)$ is the specific energy. Natural regularization by subtracting the free Hamiltonian H_0 contribution (without pairing quarks and antiquarks) has been done in the first term of Eq. (A1) because in our particular situation this normalization, in order to have the ensemble energy equal to zero at the zero pairing angle, turns out to be quite practical. It just explains the presence of a unit in the term containing $\cos\theta$.

The Hamiltonian part responsible for the interaction, $\bar{q}t^a\gamma_\mu q\bar{q}'t^a\gamma_\nu q'$, provides four nontrivial contributions. The term $\mathrm{Tr}\{\rho BB^+B'B'^+\}$ generates the following items: $\bar{V}_{\alpha i}(\mathbf{p},s)t^a_{ij}\gamma^\mu_{\alpha\beta}V_{\beta j}(\mathbf{Q},T)\bar{V}_{\gamma k}(\mathbf{Q},T)t^b_{kl}\gamma^\mu_{\gamma\delta}V_{\delta l}(\mathbf{p},s)$ (a similar term but with the changes $Q, T \to Q', T'$ which generates another primed quark current should be added) and $-2\bar{V}(\mathbf{Q},T)t^a\gamma^\mu V(\mathbf{Q}',T')\bar{V}(\mathbf{Q}',T')t^b\gamma^\mu V(\mathbf{Q},T)$. Here (as in all other following expressions) we omitted all color and spinor indices which are completely identical to those of the previous matrix element. The term $\mathrm{Tr}\{\rho BAA'^+B'^+\}$ generates the following nontrivial contributions: $\bar{V}(\mathbf{p},s)t^a\gamma^\mu U(\mathbf{q},t)\bar{U}(\mathbf{q},t)t^b\gamma^\mu V(\mathbf{p},s) - \bar{V}(\mathbf{p},s)t^a\gamma^\mu \times U(\mathbf{P},S)\bar{U}(\mathbf{P},S)t^b\gamma^\mu V(\mathbf{p},s) - \bar{V}(\mathbf{Q},T)t^a\gamma^\mu U(\mathbf{q},t)\bar{U}(\mathbf{q},t)\times t^b\gamma^\mu V(\mathbf{Q},T) + \bar{V}(\mathbf{Q},T)t^a\gamma^\mu U(\mathbf{P},S)\bar{U}(\mathbf{P},S)t^b\gamma^\mu V(\mathbf{Q},T)$. Averaging $\mathrm{Tr}\{\rho AA^+A'A'^+\}$ gives the contributions $\bar{U}(\mathbf{P},S)t^a\gamma^\mu U(\mathbf{p},s)\bar{U}(\mathbf{p},s)t^b\gamma^\mu U(\mathbf{P},S)$ (adding a similar term but with the changes $P, S \to P', S'$) and $-2\bar{U}(\mathbf{P},S)t^a\gamma^\mu U(\mathbf{P}',S')\bar{U}(\mathbf{P}',S')t^b\gamma^\mu V(\mathbf{P},S)$. Another nontrivial contribution comes from averaging $\mathrm{Tr}\{\rho A^+B^+B'A'\}$, and it has the form $\bar{V}(\mathbf{Q},T)t^a\gamma^\mu \times U(\mathbf{P},S)\bar{U}(\mathbf{P},S)t^b\gamma^\mu V(\mathbf{Q},T)$. The other diagonal matrix elements generated by the terms $\mathrm{Tr}\{\rho AA^+B'B'^+\}$, $\mathrm{Tr}\{\rho BB'^+A'^+A'\}$ do not contribute at all (their contributions are equal to zero). Similar to the calculation of the matrix elements at zero temperature performed in Ref. [5], we should carry out the integration over the Fermi sphere with the corresponding distribution functions in the quark and antiquark momenta $\int^{P_F}\frac{d\mathbf{p}}{(2\pi)^3} \to \int\frac{d\mathbf{p}}{(2\pi)^3}[n(p)+\bar{n}(p)]$ if we deal with a finite temperature. All necessary formulas for the polarization matrices which contain the traces of the corresponding spinors can be found in Refs. [4,5]. Bearing this fact in mind, here we present immediately the result for the mean energy density per one quark degree of freedom as

$$w = \int \frac{d\mathbf{p}}{(2\pi)^3}|p_4|\cos\theta[n(p)+\bar{n}(p)] + 2G\int \frac{d\mathbf{p}}{(2\pi)^3}\sin(\theta-\theta_m)[n(p)+\bar{n}(p)]\int \frac{d\mathbf{q}}{(2\pi)^3}\sin(\theta'-\theta'_m)I - G$$
$$\times \int \frac{d\mathbf{p}}{(2\pi)^3}\sin(\theta-\theta_m)[n(p)+\bar{n}(p)]\int \frac{d\mathbf{q}}{(2\pi)^3}\sin(\theta'-\theta'_m)[n(q)+\bar{n}(q)]I + +$$
$$\times \int \frac{d\mathbf{p}}{(2\pi)^3}|p_4|(1-\cos\theta) - G\int \frac{d\mathbf{p}}{(2\pi)^3}\sin(\theta-\theta_m)\int \frac{d\mathbf{q}}{(2\pi)^3}\sin(\theta'-\theta'_m)I \tag{A2}$$

(up to the constant that is unessential for our consideration here) [23]. It is quite practical to single out the color factor in the four-fermion coupling constant as $G = 2\tilde{G}/N_c$. Now performing the following transformations while integrating in the interaction terms,

$$2\int d\mathbf{p}f\int d\mathbf{q} - \int d\mathbf{p}f\int d\mathbf{q}f' - \int d\mathbf{p}\int d\mathbf{q} = \int d\mathbf{p}f\int d\mathbf{q}(1-f') - \int d\mathbf{p}(1-f)\int d\mathbf{q},$$

and changing the variables $\mathbf{p} \leftrightarrow \mathbf{q}$ in the last term, we obtain

$$\int d\mathbf{p}f\int d\mathbf{q}(1-f') - \int d\mathbf{p}\int d\mathbf{q}(1-f') = -\int d\mathbf{p}(1-f)\int d\mathbf{q}(1-f').$$

Here the primed variables correspond to the momentum q. Then, putting all the terms together we come to Eq. (11).

[1] J. Wambach, arXiv:1101.4760v1.
[2] N. Borghini, Heavy Ions at the LHC: Lessons from the First Data, Proceedings of the LHCC Meeting at CERN, 2011.
[3] V. A. Khodel, Pis'ma Zh. Eksp. Teor. Fiz. **16**, 410 (1972) [JETP Lett. **16**, 291 (1972)]; Pis'ma Zh. Eksp. Teor. Fiz.**18**, 126 (1973) [JETP Lett. **18**, 72 (1973)]; S. A. Fayans and V. A. Khodel, Pis'ma Zh. Eksp. Teor. Fiz. **17**, 633 (1973) [JETP Lett. **17**, 444 (1973)].
[4] G. M. Zinovjev and S. V. Molodtsov, Teor. Mat. Fiz. **160**, 244 (2009) [Theor. Math. Phys. **160**, 1238 (2009)]; Phys. Rev. D **80**, 076001 (2009); Europhys. Lett. **93**, 11001 (2011).
[5] S. V. Molodtsov, A. N. Sissakian, and G. M. Zinovjev, Europhys. Lett. **87**, 61001 (2009); Phys. At. Nucl. **73**, 1245 (2010).
[6] Y. Nambu and G. Jona-Lasinio, Phys. Rev. **122**, 345 (1961).
[7] T. Hatsuda and T. Kunihiro, Phys. Rep. **247**, 221 (1994).
[8] At the Fermi momenta of dynamical quark mass order.
[9] H. Tezuka, Phys. Rev. C **22**, 2585 (1980); **24**, 288 (1981).
[10] T. Matsui, Nucl. Phys. **A370**, 365 (1981).
[11] The chiral quark condensate for the filled-up state develops a quantity of about $(100\ \mathrm{MeV})^3$ (at $T = 0$) (see [5]) that demonstrates the obvious tendency of restoring a chiral symmetry.
[12] M. Asakawa and K. Yazaki, Nucl. Phys. **A504**, 668 (1989).
[13] One could observe an indirect confirmation of this hypothesis, for example, in the existing degeneracy of excited baryon states in Ref. [14].
[14] L. Ya. Glozman, Phys. Rep. **444**, 1 (2007).
[15] A similar uncertainty is present in the other predictions of chiral symmetry restoration scenarios; for example, it stretches from two to six units of the normal nuclear density.
[16] A. I. Larkin and Yu. N. Ovchinnikov, Sov. Phys. JETP **20**, 762 (1965).
[17] T. Eguchi and H. Sugawara, Phys. Rev. D **10**, 4257 (1974); K. Kikkawa, Prog. Theor. Phys. **56**, 947 (1976); M. K. Volkov, Fiz. Elem. Chastits At. Yadra **17**, 433 (1986).
[18] S. Carignano, D. Nickel, and M. Buballa, Phys. Rev. D **82**, 054009 (2010); D. Nickel, Phys. Rev. Lett. **103**, 072301 (2009); G. Basar and G. V. Dunne, Phys. Rev. Lett. **100**, 200404 (2008); T. Kunihiro, Y. Minami, and Z. Zhang, Prog. Theor. Phys. Suppl. **186**, 447 (2010).
[19] J. D. Walecka, Ann. Phys. (N.Y.) **83**, 491 (1974); F. E. Serr and J. D. Walecka, Phys. Lett. **79B**, 10 (1978).
[20] J. Boguta and A. Bodmer, Nucl. Phys. **A292**, 413 (1977).
[21] K. Huang and D. R. Stump, Phys. Rev. D **14**, 223 (1976); R. Friedberg and T. D. Lee, Phys. Rev. D **18**, 2623 (1978); R. Goldflam and L. Wilets, Phys. Rev. D **25**, 1951 (1982); E. G. Lübeck, M. C. Birse, E. M. Henley, and L. Wilets, Phys. Rev. D **33**, 234 (1986).
[22] W. Broniowski and M. K. Banerjee, Phys. Lett. **158B**, 335 (1985).
[23] It is interesting to notice that the existence of the angle θ_m stipulates the discontinuity of the mean energy functional mentioned above and discovered in [4].